

Intercalation of Poly(Ethylene Oxide) Derivatives into Layered Double Hydroxides

Fabrice Leroux,^[a] Pilar Aranda,^{*[b]} Jean-Pierre Besse,^[a] and Eduardo Ruiz-Hitzky^[b]

Keywords: Layered compounds / Intercalations / Nanostructures

Mono- and bi-functional guest molecules, poly(ethylene glycol)-*n*-alkyl-3-sulfopropyl diether (PEG-AS) and poly(ethylene glycol)dicarboxylic acid (PEG-DC), containing hydrophilic polyoxyethylene (PEO) chains of different ethylene oxide units (EOUs) are incorporated between the layers of $\text{Cu}_2\text{Cr}(\text{OH})_6\text{Cl}\cdot n\text{H}_2\text{O}$ hydrotalcite-type materials. The intercalation compounds are characterized by chemical analysis, adsorption measurements, XRD, SEM, FTIR and ^{13}C CP-MAS spectroscopy. It is found that the polyoxyethylene chain of PEG-DC distorts its helical symmetry when it is intercalated in the LDH galleries. The basal spacing of PEG-AS nan-

ocomposites is independent of the number, *n*, of EOUs in the polymer chain. In addition to changes in the IR bands, ^{13}C CP-MAS spectra are modified with new resonance peaks at more deshielded values. These facts suggest a strong interaction of polyether chains with the LDH inner-surface, with the hydrophobic alkyl tail dangling into the interlamellar space. It is shown that the terminal functionalities dictate the arrangement of the PEO chains.

(© Wiley-VCH Verlag GmbH & Co. KGaA, 69451 Weinheim, Germany, 2003)

Introduction

The preparation of hybrid organic-inorganic nanocomposites has generated a lot of interest.^[1] Layered materials are well-known to be highly suitable as host matrices for the incorporation of a large variety of organic species, readily accommodating the guest molecules via topotactic reactions. The development of tunable systems synergically enhanced by their two components is topical, the main interest being to obtain desirable properties that are unattainable from only one of the two components. This notion has also been extended to reinforced composites in which the inorganic part is usually finely dispersed or exfoliated within a polymer that supplies the mechanical strength.^[2]

Due to their applications in heterogeneous catalysis, a lot of interest has been devoted to layered double hydroxides (LDH), also known as hydrotalcite-like solids, as host materials.^[3] $\text{Mg}(\text{OH})_2$ brucite material has been used, in which the M^{2+} cations are partially substituted by M^{3+} cations. The substitution creates a positive net charge counterbalanced by the presence of anions located in the interlamellar region. The exchange capacity of LDH materials, defined by the trivalent to divalent cation ratio, is usually two to three times greater than that of cations in smectite clay minerals. This may be considered as a drawback for incorporat-

ing a large organic guest, when considering the packing between the layers. Nevertheless, large molecules with variable functionalities lying parallel to the LDH plan have been incorporated, such as DNA^[4] or polymers.^[5] It was found that the match between the charge density and the monomeric repetition of the LDH layer, viz. the projected area of the anionic function, is of great importance in obtaining complete exchange with large molecules and the ordered nanocomposites of the stiff polymer.^[5d]

With regard to the nanocomposites, a lot of attention has been paid to the intercalation of poly(ethylene oxide) (PEO) into different lamellar inorganic frameworks, such as smectites,^[6] V_2O_5 ,^[7] MoO_3 ,^[8] and other host lattices,^[9] giving hybrid materials with improved properties such as ion-conductivity or mechanical strength. PEO is known to present a flexible helical arrangement^[10] that can be distorted to obtain zigzag conformations, depending on its environment and in particular on the presence of alkali-metals or other complexing ions. Besides this application, we were also interested to know how the PEO chain could be accommodated in the LDH gallery. As intercalation in LDH hosts is limited to anionic species, we focussed our attention on two charged polymers (Table 1), one an acid monofunctional, poly(ethylene glycol)alkenylsulfonic acid (PEG-AS) and the other a bifunctional, poly(ethylene glycol)dicarboxylic acid (PEG-DC), presenting an average of 11 or 7 and 12 (OCH_2CH_2) units (EOUs), respectively.

The morphology and flexibility of layered structures are important factors for topotactic reactions. For this reason, the $\text{Cu}_2\text{Cr}(\text{OH})_6\text{Cl}\cdot n\text{H}_2\text{O}$ (noted as [CuCr] host structure) LDH sample, which is presented as corrugated sheets,^[11] is

^[a] Laboratoire des Matériaux Inorganiques, CNRS-UMR n°6002, Université Bla Pascal, 63177 Aubière cédex, France
E-mail: fleroux@chimtp-univ.bpclermont.fr

^[b] Instituto de Ciencia de Materiales de Madrid, Cantoblanco, 28049 Madrid, Spain
E-mail: aranda@icmm.csic.es

Table 1. Polyethylene oxide compounds used in this work

Polymer	Formula	Characteristics
PEG-DC	$\text{HO}_2\text{C}(\text{CH}_2\text{OCH}_2)_n\text{CO}_2\text{H}$	$n \approx 12$; Mw average 600 Dalton
PEG-AS 11	$\text{R}(\text{OCH}_2\text{CH}_2)_n\text{O}(\text{CH}_2)_3\text{SO}_3\text{K}$	$\text{R} = \text{CH}_3(\text{CH}_2)_y$, $y = 12\text{--}14$; $n \approx 11$
PEG-AS 7	$\text{R}(\text{OCH}_2\text{CH}_2)_n\text{O}(\text{CH}_2)_3\text{SO}_3\text{K}$	$\text{R} = \text{CH}_3(\text{CH}_2)_y$, $y = 12\text{--}14$; $n \approx 7$

taken as the host material. In addition, its acid character will prevent contamination by carbonate anion uptake, thus avoiding competition with polymer incorporation.

In this work we have tried several synthetic procedures to incorporate the two PEO-based polymers indicated above for the preparation of new polymer/LDH nanocomposites. The study of the adsorption and intercalation processes of both polymers between the sheets of the [CuCr] host structure and characterization of the resulting nanocomposites by a combination of technique, such as X-ray diffraction, FTIR and ^{13}C solid state NMR spectroscopy, employed to postulate models for the polymer arrangements. Some results concerning another LDH host solid, $(\text{Zn}_2\text{Cr}(\text{OH})_6\text{Cl}\cdot n\text{H}_2\text{O})$ noted as [ZnCr], will also be discussed.

Results

Polymer Incorporation

A powder X-ray diffraction pattern of [CuCr], typical of hydroxalite-type material, was refined using an $R\bar{3}m$ space group in rhombohedral symmetry (Figure 1a). The cell parameters *a* and *c* (equal to three times the interlamellar distance) are equal to 0.31 nm and 2.31 nm, respectively, in agreement with previous results.^[11]

The uptake of PEG-DC between the LDH layers is confirmed by an expansion of the *d*-spacing. The intercalation of PEG-DC performed in an aqueous medium for four hours induces an increase of the basal spacing from 0.77 to 3.03 nm (Figure 1b). Longer reaction times (up to three days) give rise to a lower *d*-spacing of 2.60 nm (Figure 1c). To explain this result it is necessary to suppose that the sample is altered by the progressive action of the solution containing PEG-DC or invoking a reorganization of the polymer chain inside the interlayer space of the LDH. This could be due to a reorganization of the polymer in the LDH galleries. An XRD pattern of the sample synthesized in butanol (BuOH) solution is very similar to the one prepared by direct exchange in an aqueous medium, although a *d*-spacing of 2.95 nm is obtained (Figure 1d). It is noteworthy that other alternatives such as the guest displacement or templating methods, appear to be unsuccessful in completing the exchange, giving rise to a mixture of an intercalated phase with a *d*-spacing of about 2.6 nm and to the pristine host material.

In comparison with the pristine host material, the broadness of the diffraction peaks is affected by the polymer incorporation. This broadening indicates the presence of

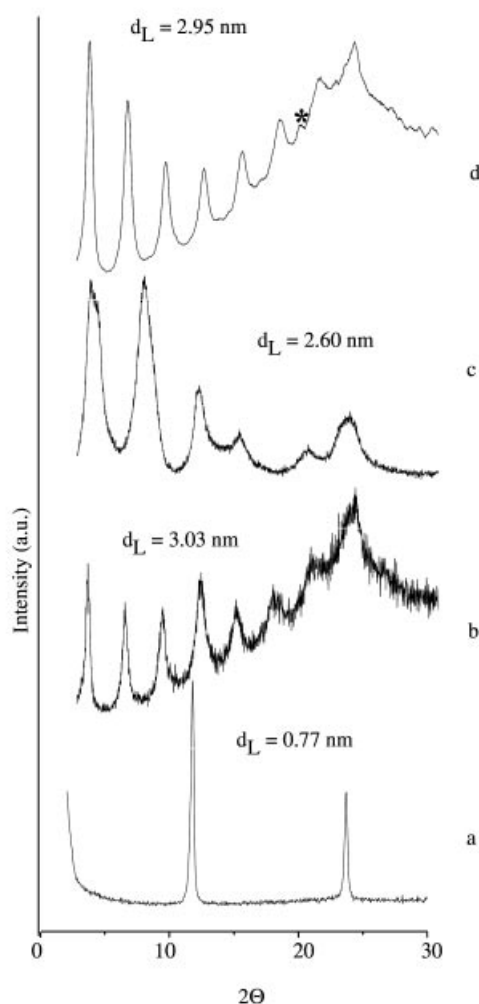


Figure 1. XRD patterns of: a) [CuCr] LDH pristine material, and PEG-DC/LDH nanocomposites obtained after b) 4 hours and c) 3 days of exchange reaction in water, and d) 4 hours of exchange reaction in butanol (* indicates a non-harmonic peak observed at 19.3° , i.e. 0.46 nm)

either some turbostatic effects or of a large decrease in the stacking sequence, as usually observed after topotactic reactions. This is even more pronounced after a longer exchange reaction time (Figure 1c). The incorporation of PEG-AS 11, by an exchange reaction, is also visible from the variation of the 2D-periodicity from 0.77 to 3.79 nm (Figure 2a). Since the diffusion of PEG-AS into the LDH gallery may be thermodynamically and/or sterically hindered, the templating method was carried out. During the co-precipitation, the polymer is entrapped between LDH sheets.

This is associated with a greater expansion of the d-spacing of up to 4.30 nm (Figure 2b). In Figure 2, the set of the first three harmonics is of different intensity. This is related to the arrangement of the organic molecule within the interlayer space. The polymer organization is then sensitive to the synthetic pathway. Additionally, a broad scattering hump is observed between 20–30° in 2 θ , suggesting that a part of the polymer remains associated with the surface of the material. This occurs because the polymer is used in excess and can be adsorbed on the surface during the co-precipitation; the use of less polymer during the formation of $\text{Cu}_2\text{Cr}(\text{OH})_6\text{Cl}\cdot n\text{H}_2\text{O}$ has not been explored.

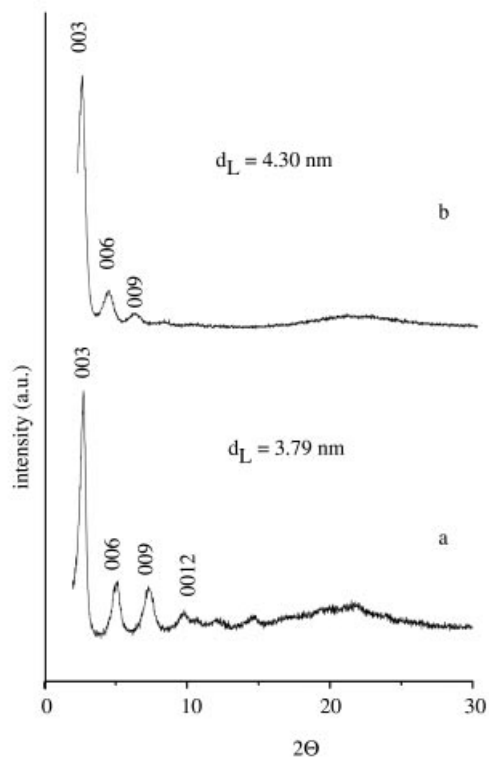


Figure 2. XRD patterns of PEG-AS (11 EOUs)/[CuCr] nanocomposites obtained via: a) exchange reaction in water, and b) co-precipitation

Our findings may be compared with the incorporation of $\text{C}_{12}\text{H}_{25}(\text{OCH}_2\text{CH}_2)_m\text{SO}_4^-$ surfactant molecules ($m = 1, 2, 4$) between LDH materials as reported by Kopka et al.^[12] The authors noticed that the degree of exchange decreased with the increase of EOUs (90 and 71% of exchange for $m = 1$ and 4, respectively) reaching a d-spacing of 3.31 nm for $m = 4$. In our case, this implies a highly constrained environment of PEG-AS 11 between LDH sheets because the d-spacing changes from 3.60 to 3.79 nm for the polymer with 7 and 11 EOUs, respectively.

It is noteworthy that for the exchange reaction, and after repeated centrifugations, the solution still remains a pale green color. This shows the presence of finely dispersed particles. Such behavior must be related to the colloidal properties of PEG-AS that induces the formation of micelles, thus giving rise to the disassembly of the LDH microcrystals.

This approach could be an alternative to other exfoliation processes.^[13]

The carbon content of the nanocomposites is lower than what was theoretically expected from the complete exchange reaction. The polymer content per formula $[\text{Cu}_2\text{Cr}(\text{OH})_6]$ is found to be in the range of 0.24–0.76 for PEG-AS and 0.53–0.84 for PEG-DC (Table 2). These differences depend strongly on the synthetic approach and may be explained by the limited diffusion of the polymer between the LDH sheets, as reported for the intercalation of cumbersome molecules.^[14] The presence of chlorine anions was detected in the material, showing that the host structure encounters a co-intercalation phenomenon. A peculiar arrangement of the EOU units may also induce strong effects (see below).

Polymer Adsorption Measurements

Adsorption isotherms (Figure 3) exhibit features characteristic of the H(2) Langmuir type according to the classification of Giles et al.;^[15] this usually occurs when the solute consists of large units such as ionic micelles or polymeric molecules. It shows that both polymers possess a strong affinity for the LDH surface, and are completely adsorbed at a low concentration range. The Langmuir-type process is modeled according to Equation (1),^[16] where C_e is the concentration of adsorbate at equilibrium (mmol/L), q_e the amount adsorbed at equilibrium (mmol/g), X_m (mmol/g) the maximum amount of adsorbate that can be adsorbed in a monolayer, and K_e the Langmuir constant related to the energy of adsorption.

$$C_e/q_e = 1/X_m K_e + C_e/X_m \quad (1)$$

The q_e versus C_e curve was fitted according to Equation (1) (inset Figure 3, a and b). The fitting and the correlation parameters for both polymers are indicated in the figure caption. X_m and K_e are equal to 0.48 and 0.37, respectively, for the adsorption process of PEG-DC, and 1.18 and 5.76, respectively, for the PEG-AS with 11 EOUs. The energy of adsorption is much higher for PEG-AS than it is for PEG-DC. This agrees with the stronger acid character of sulfonic versus carboxylic species.

It is interesting to note that the adsorption mechanism could be different for each polymer. In fact, the analysis of the shape of the plateau and the maximum adsorbed amount is quite different for each one. In both cases, the polymer must be strongly reorganized in the interlayer space, as shown by the variations in the adsorbed amount of polymer and d-spacing values.

For PEG-DC the maximum of the adsorbed amount is lower than 0.50 mmol per gram, which corresponds to 0.16 mol per formula. There is no complete ion-exchange even for the most concentrated equilibrium solutions. There is a progressive intercalation as the amount of polymer increases, and the basal spacing of the organic intercalated phase is modified. The maximum adsorption has not been reached and so even for the 0.46 mmol/g material there are

Table 2. Characteristics of PEG-DC/ and PEG-AS/ nanocomposites prepared in this work

Nanocomposites	Method of synthesis	Δd_L (nm)	%C in the solid	Tentative formula ^[a]
PEG-DC/CuCr	ion-exchange in H ₂ O	2.55	17.3	Cu ₂ Cr(OH) ₆ ·PEG-DC _{0.32} Cl _{0.36} ·nH ₂ O
	ion-exchange in BuOH	2.47	29.5	Cu ₂ Cr(OH) ₆ PEG-DC _{0.76} ·nH ₂ O ^[c]
	co-precipitation	2.12 ^[b]	14.6	Cu ₂ Cr(OH) ₆ PEG-DC _{0.24} Cl _{0.52} ·nH ₂ O
PEG-AS/CuCr	ion-exchange of PEG-AS 11 EOUs in H ₂ O	3.31	30.1	Cu ₂ Cr(OH) ₆ PEG-AS _{0.53} Cl _{0.47} ·nH ₂ O
	ion-exchange of PEG-AS 7 EOUs in H ₂ O	3.12	33.5	Cu ₂ Cr(OH) ₆ PEG-AS _{0.70} Cl _{0.30} ·nH ₂ O
	co-precipitation in presence of PEG-AS 11 EOUs	3.82	36.2	Cu ₂ Cr(OH) ₆ PEG-AS _{0.84} Cl _{0.16} ·nH ₂ O
PEG-AS/ZnCr	ion-exchange of PEG-AS 11 EOUs in H ₂ O	3.22	33.1	Zn ₂ Cr(OH) ₆ PEG-AS _{0.66} Cl _{0.34} ·nH ₂ O
	ion-exchange of PEG-AS 7 EOUs in H ₂ O	3.07	32.3	Zn ₂ Cr(OH) ₆ PEG-AS _{0.65} Cl _{0.35} ·nH ₂ O

^[a] Tentative formula calculated assuming that the anionic polymers are intercalated by replacing Cl[−] ions of the pristine Cu₂Cr(OH)₆Cl·nH₂O or Zn₂Cr(OH)₆Cl·nH₂O LDH matrices. ^[b] Also a phase of pristine LDH is observed. ^[c] Incorporated amount of PEG-DC exceeds the ion-exchange capacity.

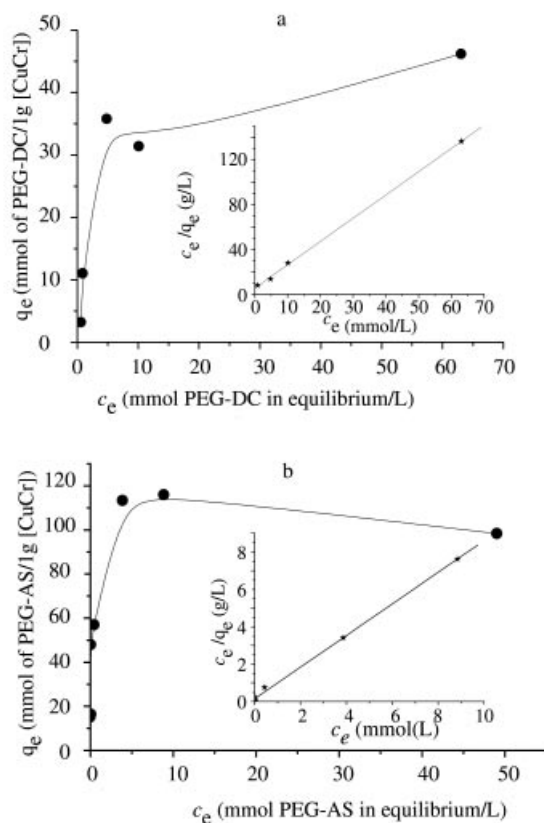


Figure 3. Adsorption isotherm from water solutions of: a) PEG-DC and b) PEG-AS containing 11 EOUs on [CuCr]; the fit is displayed in the inset [according to Equation (1)]: a) $C_e/q_e = 5.55 + 0.0033292 C_e$ ($R = 0.99968$), b) $C_e/q_e = 0.1468 + 0.00109 C_e$ ($R = 0.9989$)

still peaks associated with the pristine solid [CuCr]. An incorporation of PEG-DC as high as 0.76 mol per [CuCr] formula unit is reached using BuOH as the solvent

(Table 2). Such high polymer content may be explained by the preparation method. The use of BuOH under reflux conditions is known to break up the LDH structure, thus creating an increase in the interface. A part of the polymer must coat the surface of the crystallites.

For the PEG-AS (11 EOUs) there is a maximum in the adsorption close to 120 mmol/g (0.40 mmol per formula unit) for equilibrium concentrations below 20 mmol/L. At higher C_e values, a slight decrease is observed for the adsorbed amount of about 0.35 mol per formula unit. The XRD patterns still exhibit the diffraction peak of pristine [CuCr] LDH material. The formation of an intercalated phase progresses along with an increase in the amount of polymer to the point where the LDH structure starts to dissolve, as illustrated by the large scatter between 20 and 30° in 2 θ . A green color indicates that a disassembly of the 2D-host matrix occurs, probably entangled by the polymer. The monofunctional polymer may play the role of a spacer acting at the edge of the crystallites like dodecylsulfate molecules for the LDH delamination.^{[13a][13b]}

FTIR Spectroscopy

IR spectroscopy of the resulting PEO/LDH nanocomposites affords significant information on how the polymer is associated into the 2D host solid. The lattice vibration bands arising from M–O and O–M–O (M = Cu, Cr) bonds are observed in the 400–800 cm^{−1} region and there are no important differences between LDH and the nanocomposites (Figure 4 and 5). In the 1300–1350 cm^{−1} region several vibration bands appear that are related to the wagging vibration of the –CH₂–O– groups, which give crucial information about characteristics of the polyoxyethylene skeleton and its deformation. This is exemplified by the vibration band at 1346 cm^{−1} for PEG-DC (Figure 4), characteristic of –CH₂–O– groups of polyether chains in a helical conformation. The presence of a weak band at 1325

cm^{-1} in the non-intercalated pristine polymer suggests a very slight distortion of the helix. However, for the PEG-DC/LDH nanocomposites the band at higher wavenumber can be shifted towards 1330 cm^{-1} and a new and intense band develops at 1314 cm^{-1} . These facts indicate that the polyoxyethylene chain presents EOUs in a *trans* conformation^[10] and therefore the helix is distorted. The degree of distortion depends on the nature of the host-guest matrix interactions. Some of the nanocomposites show planar zig-zag conformations of the polymer as is observed for other poly(ethylene oxide) intercalation compounds.^[6]

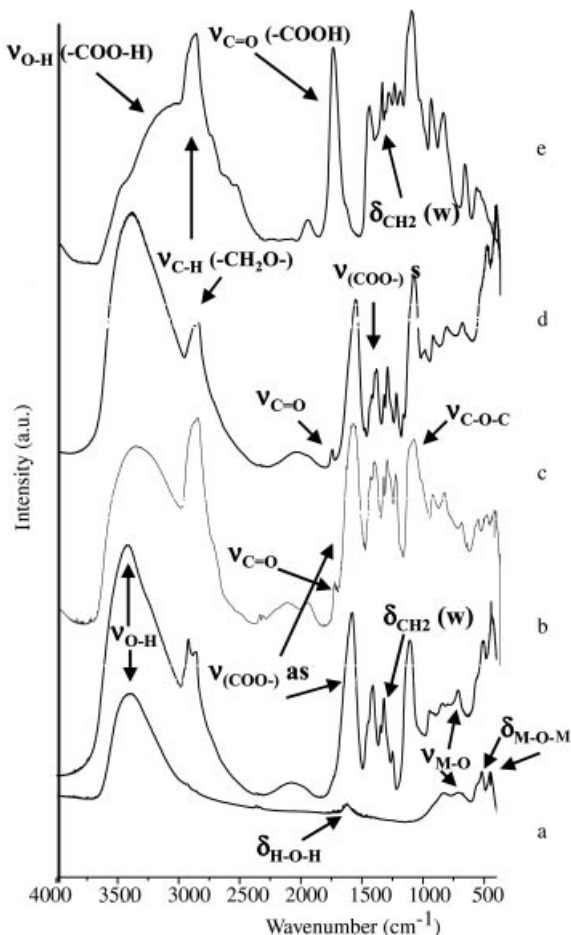


Figure 4. FTIR spectra of: (a) LDH pristine material, and PEG-DC/LDH nanocomposites obtained via b) ion-exchange in water, c) ion-exchange in butanol, d) co-precipitation, and e) pure PEG-DC.

The assignment of the different vibration bands is displayed in Table 3. In the case of PEG-DC based nanocomposites, the bands associated with the $\nu_{\text{C=O}}$ stretch of the carboxylic groups are split into two at around 1578 cm^{-1} and 1407 cm^{-1} , corresponding to the antisymmetric and symmetric $\nu_{\text{C=O}}$ mode of the COO^- groups, respectively, as the acid is intercalated in the anionic form. In spite of this, the spectra of the nanocomposites, prepared by co-precipitation and BuOH under reflux, still show weak bands at around 1770 cm^{-1} and 1240 cm^{-1} , indicating the presence

of free acid groups in the polymer associated with the solid.

The $\nu_{\text{O=S=O}}$ vibration bands of the SO_3^- group are observed at around the same wavenumber, 1190 and 1040 cm^{-1} for the antisymmetric and symmetric contribution, respectively, for pure PEG-AS and PEG-AS/LDH nanocomposites (Figure 5). The inversion in their relative intensity suggests that the SO_3^- group is in a more symmetric environment for the nanocomposites; this is probably a consequence of the interaction with the hydroxide sheet. For PEG-AS (11 EOUs)/LDH nanocomposites prepared by different synthetic approaches, either in [CuCr] or [ZnCr] LDHs, the striking difference when compared with the pristine polymer or even with the nanocomposites based on PEG-AS of 7 EOUs, is the appearance of two new bands around 1720 and 1570 cm^{-1} (Figure 5). The assignment of these bands is still unclear as there are no appreciable alterations, either in the organic backbone vibration bands or in those corresponding to the inorganic host (Figure 4). The vibration band at around 1720 cm^{-1} is indicative of a carbonyl group, suggesting that the polymer chain can be partially altered by heterolytic oxidation reactions.

¹³C Solid-State NMR Spectroscopic Study

In order to get more information on the guest/host interaction in the PEG-AS/[CuCr] nanocomposite, ¹³C solid-state CP MAS spectroscopy experiments were performed (Figure 6). The spectrum of PEG-AS of 11 EOUs exhibits several resonance peaks, with chemical shifts attributed as follows: $\delta = 72.2\text{ ppm}$ to carbon nuclei in the $(-\text{OCH}_2\text{CH}_2-)$ ethylene oxide chain, $\delta = 48.4\text{ ppm}$ for C attached to an SO_3^- group, and several peaks lumped together (shoulder Figure 6a) from $\delta = 30.2$ to $\delta = 14.4\text{ ppm}$ associated with the different methylene groups, and the terminal CH_3 , respectively. The latter contribution is also observed for the LDH derivatives (Figure 6b and c), only the response is broader. For the C linked to the S, an up-field shift is observed up to $\delta = 42.5\text{ ppm}$; this shielding may correspond to an electrostatic attraction between the molecule and the sheets of [CuCr] as observed in other systems.^[17] The same effect, but much less pronounced, is observed for carbon nuclei in the ethylene chain with a shielding from $\delta = 72.2$ to 71.1 ppm . However, it is interesting to note that the relative carbon nuclei population of the polymer is very different from that of the organic-inorganic phase. Even if the CP experiment does not strictly supply quantitative information, it is obvious that the population relative to carbon in the polyoxyethylene chain has decreased.

Surprisingly, some new peaks at $\delta = 127.0$, 121.9 and 149.8 ppm appear for the nanocomposite that are absent for PEG-AS. These are not spinning side-bands since they are present in the spectra recorded at the two different fields. Such chemical shift values are typical of aromatic or highly deshielded carbons such as carbonyl carbons. It is noteworthy that these down-field contributions are not observed for PEG-DC hybrid materials.

Table 3. IR vibration bands (cm^{-1}) and their assignment for the PEG-DC and PEG-AS polymers and some of their LDH nanocomposites derivatives

PEG-DC	PEG-DC/CuCr ion-exchange	PEG-DC/CuCr co-precipitation	PEG-AS (11 EOUs)	PEG-AS (11 EOUs)/CuCr ion-exchange	PEG-AS (11 EOUs)/CuCr co-precipitation	PEG-AS (11 EOUs)/ZnCr ion-exchange	PEG-AS (7 EOUs)/CuCr ion-exchange	Assignment ^[a]
$\approx 3200^{[b]}$	3414	3406		3436	3422	3464	3442	$\nu_{\text{O-H}}$ $\nu_{\text{O-H}} (-\text{COO-H})$
2878	2864	2870	2914	2920	2914	2918	2918	$\nu_{\text{C-H}} (-\text{CH}_2-)$
1742		1771	2858	2848	2850	2848	2846	$\nu_{\text{C-H}} (-\text{CH}_2-\text{O}-)$
				1724	1760 ^[c] , 1718 ^[c]	1724 ^[c]		$\nu_{\text{C=O}} (\text{COOH})$
	1578	1578		1618	1620		1621	$\delta_{\text{HOH}} (\text{H}_2\text{O})$
			1462	1570 ^c	1570 ^[c]	1574 ^[c]		$\nu_{\text{C=O}} (\text{COO}^-) \text{ asym}$
	1407	1407		1456	1450	1456	1457	$\delta_{\text{CH}_2} \text{ w } (-\text{CH}_2-)$
1346 m	1332 w	1350 w	1342	1344	1344	1344	1346	$\nu_{\text{C=O}} (\text{COO}^-) \text{ sym}$
1325 w	1314 m	1314 m						$\delta_{\text{CH}_2} \text{ w } (-\text{CH}_2-\text{O}-\text{CH}_2-)^{[d]}$
1242	1243	1242	1276		1288	1294		$\delta_{\text{CH}_2} \text{ t}$
			1188	1182	1192	1182	1186	$\nu_{\text{O=S=O}} \text{ asym } (-\text{SO}_3^-)$
				1146 ^c	1150 ^[c]	1140 ^[c]	1150 ^[c]	$\nu_{\text{C-O}}^{[c]}$
1104	1102	1100	1100	1100	1112	1112	1110	$\nu_{\text{C-O-C}} \text{ asym}$
			1058, 1038	1038	1041	1038	1038	$\nu_{\text{O=S=O}} \text{ sym } (-\text{SO}_3^-)$
942	936	940	948	945	948	942	942	$\nu_{\text{CH}_2} \text{ r}$
			840	850	851		865	$\nu_{\text{S=O}} (-\text{SO}_3^-)$
				790 ^c		788 ^[c]	790 ^[c]	$\nu_{(\text{COO}-)} \text{ formate}$
	707	707		735		731	728	$\nu_{\text{M-O}}$
					570	574		$\nu_{\text{C-S}}$
	504, 432	500, 436		508, 434	506, 428	506, 380	510, 436	$\delta_{\text{O-M-O}}$

^[a] Asym: antisymmetric; sym: symmetric; w: wagging; t: twisting; r: rocking. ^[b] Very broad and strong band centred around 3200 cm^{-1} .

^[c] Tentative assignation of the bands to vibration modes of C=O functions related to oxidation products of the oxyethylene polymer chain. ^[d] When two bands are observed the relative intensity of both of them is signalled (m = medium; w = weak).

SEM Observations

SEM pictures of the pristine material and derivative phases are displayed in Figure 7. The starting chloride-exchanged [CuCr] material gives rise to a platelet-like shape, this morphology being characteristic of the applied method of synthesis.^[5b] This is found to be different for the PEG-DC nanocomposites, which show a leaf aspect.

For PEG-AS/LDH nanocomposites with either 7 or 11 EOUs, the crystallite surface presents a crumpled shape. The part of the polymer coating the material (see above) must be the origin of the irregularities. Moreover, the polymer chains must be linked to close chunks, giving rise to a large ill-defined piece. In the inset of Figure 7 (see f), the 2D-character is evidenced for these hybrid organic-inorganic phases.

Discussion

To shed some light on the present results, different hypotheses must be considered in order to postulate a model for the intercalated materials. The conformation of the PEO chain is an important factor for the polymer geometry between the layers. PEO presents a repetition of $(-\text{OCH}_2\text{CH}_2-)$ units adopting a helical structure in its crystalline state.^[10] Instead of taking the EOU linear size as three methylene groups in a zigzag conformation,^[12] a flexible polyoxyethylene chain adopting a helix with either a $9_{1/2}$ or $7_{1/2}$ symmetry must be considered for long PEO chains.^[10] The first

gives rise to a dimension of 1.95 nm for 9 EOUs, and the second 1.90 nm for 7 EOUs.

By subtracting the LDH layer width of 0.48 nm from the d-spacing, we access the space available to accommodate the polymer between the sheets. For the PEG-DC nanocomposite prepared by ion-exchange, this gives a space of around 2.60 nm (Table 2), which is in agreement with a polyoxyethylene chain in a $9_{1/2}$ helical symmetry (expected value of 2.72 nm considering 12 EOUs instead of 9 in the helical conformation with the size of the two carboxylic groups being $0.12 \text{ nm}^{[14]}$). After a longer reaction time, the gallery size is shortened to 2.17 nm (Figure 1, c), showing that the polyoxyethylene chains are strongly confined and the helix is distorted by chain-chain interactions and/or with OH from the LDH layer or H_2O molecules. This interpretation is supported by the high intensity of the $\delta_{\text{CH}_2} (\text{w})$ vibration band at 1314 cm^{-1} (Table 3).

For the PEG-DC/[CuCr] nanocomposite prepared by an exchange reaction in BuOH, eight well-defined harmonics are observed suggesting that the stacking is good. An additional peak at 19.3° ($d = 0.46 \text{ nm}$) is also observed. In the absence of other possible explanations, this was related to a superlattice ($\sqrt{3}$ times the perpendicular distance between [100] planes).^[18] Since this material presents an excess of polymer over the ion-exchange capacity determined from the chemical analysis (Table 2), a portion of the organics should be intercalated either in their acid form and/or adsorbed on the surface through interaction with OH groups. The first interpretation is supported by the presence of a

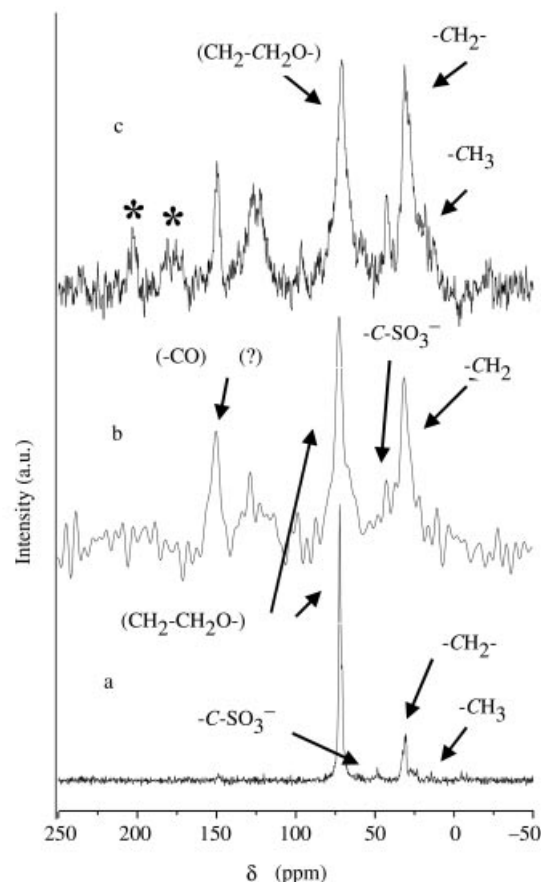


Figure 6. ^{13}C NMR spectra of: (a) the potassium salt of PEG-AS of 11 EOUs, and the PEG-AS/[CuCr] nanocomposites recorded at (b) 7.04 T (300 MHz), and c) 9.39 T (400 MHz); spinning sidebands are indicated with an asterisk.

The same approach was taken to unravel the arrangement, between the LDH sheets, of the PEG-AS with 11 EOUs. Using similar calculations for the organic moieties, the size of the polymeric molecule is 4.73 and 5.39 nm, depending on the $9_{1/2}$ or $7_{1/2}$ helical symmetry, respectively. This calculation was made considering the following dimensions from Kopka and co-workers:^[12] 0.127 nm per CH_2 group, and 0.30 nm for the $-\text{CH}_3$ and 0.18 nm for the

The FTIR spectra of PEG-AS/LDH nanocomposites show only a band at around 1345 cm^{-1} , which is assigned to the δ_{CH_2} (w) vibration mode of the EOUs in the helical conformation; this is different from that of the PEG-DC/LDH derivatives. However, from ^{13}C CP MAS and FTIR spectroscopy, highly deshielded carbon atoms were observed in these latter nanocomposites compared to the polymer alone. This was also associated with the appearance of a new vibration at 1720 cm^{-1} , and may be interpreted as a strong interaction of some of the EOUs with the LDH sheets. This situation was also observed for other organic surfactants, where ethoxy groups were found to be folded in a “hairpin” conformation and remained in contact with

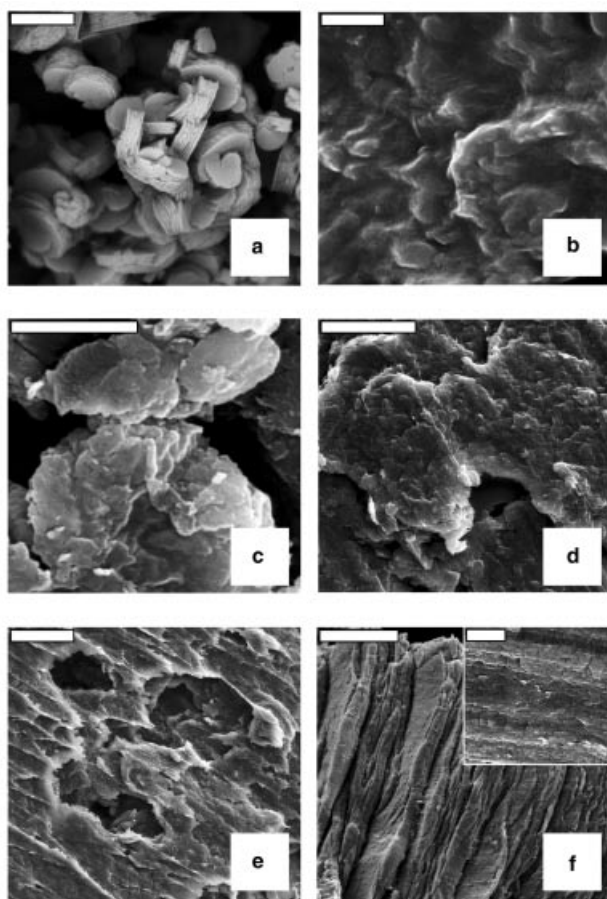


Figure 7. SEM pictures of (a) [CuCr] LDH pristine material; PEG-DC/[CuCr] nanocomposites obtained via (b) ion-exchange in water, (c) co-precipitation, and PEG-AS/[CuCr] nanocomposites of the polymer of 11 EOUs prepared via (d) ion-exchange in water, (e) co-precipitation, and the polymer of 7 EOUs prepared via (f) ion-exchange in water (in inset, the view is perpendicular to the stacking direction). The bar represents 2, 2, 10, 20, 50, 5 (inset) μm , respectively

the LDH surface.^[12] However, as PEO and PEO-salt complexes in certain circumstances can easily be oxidized following different mechanisms,^[19] giving a complex mixture of primary products including ester, aldehyde, carboxylic acid and formate-end groups, the IR absorption bands observed in the $1500\text{--}1900\text{ cm}^{-1}$ region could be attributed to the oxidative degradation of the polymer catalyzed by the host LDH. Thus, for instance, the band at around 1720 cm^{-1} developed from the intercalates of PEG-AS of 11 EOUs (Table 3) could be ascribed to the formation of formate end-functions ($-\text{CH}_2\text{--O--CHO}$).

To corroborate this interpretation, PEG-AS of 7 EOUs was intercalated into [CuCr] and [ZnCr] LDH frameworks. These are materials that present the same layer charge density. From the XRD patterns (Figure 9) of nanocomposites derived from the polymer with 11 EOUs intercalated by ion-exchange in the two hosts, the space available for the guest molecule, calculated from the third harmonic position, varies from 3.31 to 3.22 nm for [CuCr] and [ZnCr] derivatives, respectively (Table 2). Thus, PEG-AS may also

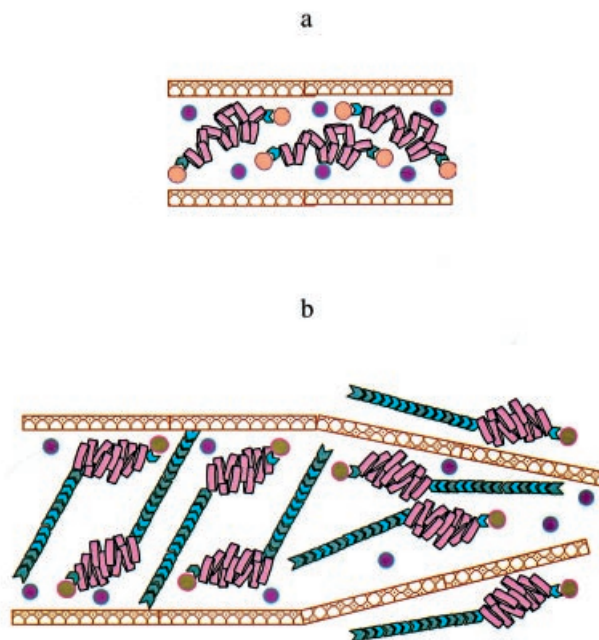


Figure 8. Proposed models for the [CuCr] LDH nanocomposites incorporating (a) PEG-DC and (b) PEG-AS

adopt a highly confined arrangement within the layers of the [ZnCr] LDH structure. For the polymer with 7 EOUs, the situation is slightly modified to 3.12 and 3.07 nm, respectively (Table 2).

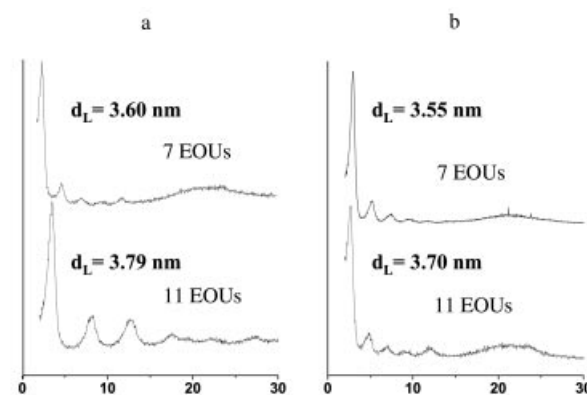


Figure 9. XRD patterns of nanocomposites prepared by ion-exchange reaction of PEG-AS of different EOUs (n) with (a) [CuCr] and (b) [ZnCr]; the values of n are displayed

The small difference between the variation of basal spacing from 7 to 11 EOUs for the PEG-AS/LDH nanocomposites cannot be explained by the increase in size of the polyoxyethylene chain. This fact proves that the polyoxyethylene chains are not directly contributing to the expansion of the interlayer space available for the molecule. These results are supported by a model in which the polyether chain interacts with the corrugated [CuCr] LDH inner-surface, with the alkyl tails dangling in the interlayer space

(Figure 8b). Qualitatively, this is the same as a polymer literally gluing the inner and outer surface of the matrix, as illustrated by SEM micrographs (Figure 7) and as pointed out by the adsorption measurements, which indirectly give rise to a large surface covered by the mono-functional guest molecule. The existence of such an interaction might also be the cause of a break in the polyether chain that originates, in certain cases, in the presence of carbonyl functions, as deduced from IR and NMR spectroscopic studies and consistent with the observations of other authors.^[19]

Conclusion

This paper provides clear evidence of the intercalation of the mono- and bifunctional molecules, PEG-DC and PEG-AS polymers, containing flexible oxyethylene groups between the sheets of LDH [CuCr]. For the macromolecule PEG-DC, the basal spacing of the hybrid phase is small, and has to be explained by assuming a highly distorted helical situation for the polyoxyethylene chain. For PEG-AS, the polymer chain must be in a helical symmetry, although complementary results gathered by FTIR and NMR spectroscopy seem to indicate the presence of additional intricate effects. From these results, we assume that the polyether chain must interact strongly with the LDH layers, giving rise to a distribution of chemical shifts depending on the orientation of the helix with the positively charged layers.

Experimental Section

All the reagents are of analytical grade: $\text{CuCl}_2 \cdot 2\text{H}_2\text{O}$, CuO , $\text{CrCl}_3 \cdot 6\text{H}_2\text{O}$, ZnCl_2 , NaOH and BuOH are commercial products from Aldrich. Water soluble polymers (Table 1), potassium poly(ethylene glycol) (ca. 7 and 11 ethylene oxide units, EOUs) $-\text{[n-alkyl(C}_{13}\text{--C}_{15})\text{--(3-sulfo} \text{propyl diether)] salt [R(OCH}_2\text{CH}_2\text{)}_n\text{O(CH}_2\text{)}_3\text{SO}_3\text{]K}$, noted as PEG-AS- n of 7 or 11 EOUs, respectively], poly(ethylene glycol)dicarboxylic acid $[\text{HO}_2\text{C(CH}_2\text{OCH}_2\text{)}_n\text{CO}_2\text{H}$, average M_n 600, $n \approx 12$ EOUs – noted as PEG-DC] are available from Aldrich. Deionized water was used for the synthesis and washing procedures.

LDH starting material, [CuCr] of general composition $\text{Cu}_2\text{Cr(OH)}_6\text{Cl} \cdot n\text{H}_2\text{O}$ was prepared by either co-precipitation or salt-oxide methods.^[20] For the former, the solutions of transition metal chlorides were slowly added at a controlled pH of 4.9 (CuCl_2 : 10^{-2} M, CrCl_3 : 5×10^{-3} M).^[20a] For the second preparation, CrCl_3 was added to a solution containing CuO that was finely dispersed in water by sonication.^[20b] The resulting precipitates were kept overnight in the mother liquor for aging, then separated by three repeated washing/centrifugation cycles and, finally, dried in air at room temperature. In the present study, the second method was preferred, giving rise to more crystalline materials. Co-precipitation was used for the templating reaction (see below). $\text{Zn}_2\text{Cr(OH)}_6\text{Cl} \cdot n\text{H}_2\text{O}$ LDH material, noted as [ZnCr], was prepared by the co-precipitation method at a constant pH of 5.5.

Intercalation of the Polymers

1) Direct exchange was performed as follows: the LDH material (30 mg) was ultrasonicated (5 minutes) in decarbonated water (25

mL) and added to a solution containing the polymer neutralized at pH 7. The amount of dissolved polymer corresponded to two to five times the anionic exchange capacity (AEC) of the LDH material (270 mequiv. per 100 g for [CuCr]). The exchange reaction was performed under nitrogen gas for 3 to 12 h. The resulting powder was centrifuged, washed several times and finally dried at room temperature. In some cases, a mixture of solvents [such as $\text{H}_2\text{O}/\text{MeOH}, \text{H}_2\text{O}/\text{EtOH}$ (1:1)] was used instead of pure water.

2) The method defined as “solvent-assisted preparation”, consists of dispersing the LDH sample into butanol. The exchange was then carried out under reflux conditions at 90 °C with vigorous stirring.

3) Co-precipitation is an approach similar to the “templating” method used by Oriaki et al.^[5b] for the incorporation of polysulfonated polymers. The hybrid LDH phase was synthesized in the presence of the polymer previously dissolved in aqueous solution (the amount of polymer corresponds to twice the AEC of the solid which, hypothetically, results in the complete formation from the initial salts concentration) on adjusting the pH to 7.0.

The adsorption isotherms were measured by the batch equilibration technique. Thus, a known amount of hydrotalcite-like material (ca. 50 mg) was sonically dispersed in 25 mL of deionized water and then kept in contact with the polymer solution at 25 °C for 24 h. The polymer concentration ranged from 10^{-4} to 5×10^{-2} M. The amount of organic matter adsorbed by the solid, expressed in mmol per gram of LDH (q_e), was determined from HCN elemental microanalyses. The final concentration (C_e , adsorbate concentration at equilibrium after a contact time of 24 hours) was determined by subtracting the quantity of polymer (m) retained by the solid from the total content in the original solution: $C_e = (C_i \times V - q_e \times m)/V$. The adsorption isotherms were obtained by plotting q_e versus C_e (relative error < 1%).

Elemental chemical analysis of the LDH materials was performed using the inductive conduction plasma coupled to atomic emission spectroscopy (ICP/AES) at Center d'Analyse de Vernaison, France. The organic content was determined by conventional HCN chemical analysis (Perkin–Elmer 240C). Materials were characterized by the XRD technique with a D500 Siemens or a Philips 1710 spectrometer, both operating with Cu-K_α radiation. FTIR was performed with a Nicolett 20SXC apparatus employing the KBr dilution technique for solid samples. SEM observations were performed on a SEM-EDX microscope (Zeiss DSM 960) operating at 15.0 kV. ^{13}C solid-state NMR spectroscopy experiments were performed with a 300 Bruker spectrometer at 75.47 MHz, using a 4-mm diameter zirconia rotor and working under magic angle spinning (MAS) condition of 10 kHz. A second spectrometer 400 Bruker (^{13}C Larmor frequency of 100.63 MHz) was also employed. ^{13}C spectra obtained by the proton-enhanced cross-polarization method (CP) were referenced to the carbonyl of the glycine calibrated at $\delta = 176.03$ ppm or tetramethylsilane (TMS).

Acknowledgments

The authors would like to thank Pr. C. Forano for fruitful discussions and Dr. I. Sobrados and Mr. F. Pinto for helpful assistance in the NMR spectroscopic study and SEM characterization, respectively. F. L. and P. A. thank the CNRS and CSIC for a French–Spanish cooperation grant (France n°7945, Spain 2000FR0024) and to the CICYT (Spain, MAT2000-1585-C03-01 and MAT2000-1451 projects) for financial support.

[1] [1a] S. Komarni, *J. Mater. Chem.* **1992**, 2, 1219–1230. [1b] E. Ruiz-Hitzky, *Adv. Mater.* **1993**, 5, 334–340. [1c] E. Giannelis,

- Adv. Mater.* **1996**, 8, 29–35. ^[1d] B. M. Novak, *Adv. Mater.* **1993**, 5, 422–433. ^[1e] G. Lagaly, *Appl. Clay Sci.* **1999**, 15, 1–9.
- ^[1f] *Polymer-Clay Nanocomposites* (Eds.: T. J. Pinnavaia & G. W. Beall), John Wiley & Sons, West Sussex, **2000**.
- ^[2] ^[2a] E. Ruiz-Hitzky, *Mol. Cryst. Liq. Cryst.* **1988**, 161, 433–452. ^[2b] Z. Wang, T. Lan, T.J. Pinnavaia, *Chem. Mater.* **1996**, 8, 2200–2204. ^[2c] J. Bujdak, E. Hackett, E. P. Giannelis, *Chem. Mater.* **2000**, 12, 2168–2174.
- ^[3] A. Vaccari, *Applied Clay Science* **1999**, 14, 161–198.
- ^[4] J.-H. Choy, S.-Y. Kwak, J.-S. Park, Y.-J. Jeong, J. Portier, *J. Am. Chem. Soc.* **1999**, 121, 1399–1400.
- ^[5] ^[5a] P. B. Messersmith, S. I. Stupp, *Chem. Mater.* **1995**, 7, 454–460. ^[5b] C. O. Oriakhi, I. V. Farr, M. M. Lerner, *J. Mater. Chem.* **1996**, 6, 103–107. ^[5c] S. Rey, J. Mérida-Robles, K.-S. Han, L. Guerlou-Demourgues, C. Delmas, E. Duguet, *Polym. Int.* **1999**, 48, 277–282. ^[5d] F. Leroux, J.-P. Besse, *Chem. Mater.* **2001**, 13, 3507–3515.
- ^[6] ^[6a] P. Aranda, E. Ruiz-Hitzky, *Adv. Mater.* **1990**, 2, 545–547. ^[6b] P. Aranda, E. Ruiz-Hitzky, *Chem. Mater.* **1992**, 4, 1395–1403. ^[6c] P. Aranda, E. Ruiz-Hitzky, *Appl. Clay Sci.* **1999**, 15, 119–135.
- ^[7] ^[7a] Y.-J. Liu, D. C. DeGroot, J. L. Schindler, C. R. Kannewurf, M. G. Kanatzidis, *Chem. Mater.* **1991**, 3, 992–994. ^[7b] E. Ruiz-Hitzky, P. Aranda, B. Casal, *J. Mater. Chem.* **1992**, 2, 581–582. ^[7c] Y.-J. Liu, J. L. Schindler, D. C. DeGroot, C. R. Kannewurf, W. Hirpo, M. G. Kanatzidis, *Chem. Mater.* **1996**, 8, 525–534.
- ^[8] ^[8a] L. F. Nazar, H. Wu, W. P. Power, *J. Mater. Chem.* **1995**, 5, 1985–1993. ^[8b] L. Wang, J. Schindler, C. R. Kannewurf, M. G. Kanatzidis, *J. Mater. Chem.* **1997**, 7, 1277–1283.
- ^[9] ^[9a] E. Ruiz-Hitzky, P. Aranda, *Anales Química Int. Ed.* **1997**, 93, 197–212. ^[9b] E. Ruiz-Hitzky, P. Aranda, in *Polymer-Clay Nanocomposites* (Eds.: T. J. Pinnavaia & G.W.Beall), John Wiley & Sons, West Sussex **2000**, pp. 19–46.
- ^[10] ^[10a] W. H. T. Davison, *J. Chem. Soc.* **1955**, 3270–3275. ^[10b] H. Tadokoro, Y. Chatani, T. Yoshihara, S. Tahara, S. Murahashi, *Makromol. Chem.* **1964**, 73, 109–127. ^[10c] B. L. Papke, M. A. Ratner, D. F. Shriver, *J. Phys. Chem. Solids* **1981**, 42, 493–500.
- ^[11] H. Roussel, V. Briois, E. Elkaïm, A. de Roy, J.-P. Besse, *J. Phys. Chem. B* **2000**, 104, 5915–5923.
- ^[12] H. Kopka, K. Beneke, G. Lagaly, *J. Colloid Interface Sci.* **1988**, 123, 427–436.
- ^[13] ^[13a] M. Adachi-Pagano, C. Forano, J.-P. Besse, *Chem. Com.* **2000**, 91–92. ^[13b] F. Leroux, M. Adachi-Pagano, M. Intissar, S. Chauvière, C. Forano, J.-P. Besse, *J. Mater. Chem.* **2001**, 11, 105–112. ^[13c] T. Hibino, W. Jones, *J. Mater. Chem.* **2001**, 11, 1321–1323.
- ^[14] M. Meyn, K. Beneke, G. Lagaly, *Inorg. Chem.* **1990**, 29, 5201–5207.
- ^[15] C. H. Giles, T. H. MacEwan, S. N. Nakhwa, D. Smith, *J. Chem. Soc.* **1960**, 3973–3993.
- ^[16] ^[16a] R. Calvet, *Environmental Health Perspectives* **1989**, 83, 145–177. ^[16b] Y. Yu, Y.-Y. Zhuang, Z.-H. Wang, *J. Colloid Inter. Sci.* **2001**, 242, 288–293. ^[16c] F. A. Banat, B. Al-Bashir, S. Al-Ashed, O. Hayajneh, *Environ. Pollution* **2000**, 107, 391–398.
- ^[17] ^[17a] Y. Komori, K. Sugahara, K. Kuroda, *Chem. Mater.* **1999**, 11, 3081–3085. ^[17b] E. M. Moujahid, J. Inacio, J.-P. Besse, F. Leroux, *J. Mater. Chem.* **2002**, 12, 3324–3330.
- ^[18] ^[18a] M. Vucelic, G. D. Moggridge, W. Jones, *J. Phys. Chem.* **1995**, 99, 8328–8337. ^[18b] A. S. Bookin, V. I. Cherkashin, V.A. Drits, *Clays Clay Miner.* **1993**, 41, 558–564.
- ^[19] ^[19a] L. Costa, A.M. Gad, G. Camino, *Macromolecules* **1992**, 25, 5512–5518. ^[19b] C. Wilhelm, J.-L. Gardette, *Polymer* **1998**, 39, 5973–5980. ^[19c] S. Morlat, J.-L. Gardette, *Polymer* **2001**, 42, 6071–6079.
- ^[20] ^[20a] S. Miyata, *Clays Clay Miner.* **1983**, 31, 305–311. ^[20b] A. De Roy, C. Forano, K. El Malki, J.-P. Besse, in *Synthesis of Microporous Materials Vol. II. Expanded Clays and Other Microporous Solids* (Eds.: L. Occelli, H. Robson), Van Nostrand Reinhold, New York, **1992**, pp. 108–169.

Received June 19, 2002
[I02325]